The Annals of Applied Statistics
2014, Vol. 8, No. 3, 1782–1799
DOI: 10.1214/14-AOAS756

INCORPORATING GEOSTROPHIC WIND INFORMATION FOR IMPROVED SPACE–TIME SHORT-TERM WIND SPEED FORECASTING[1]

BY XINXIN ZHU[2,*], KENNETH P. BOWMAN[*] AND MARC G. GENTON[2,†]

Texas A&M University[*] and King Abdullah University of Science and Technology[†]

Accurate short-term wind speed forecasting is needed for the rapid development and efficient operation of wind energy resources. This is, however, a very challenging problem. Although on the large scale, the wind speed is related to atmospheric pressure, temperature, and other meteorological variables, no improvement in forecasting accuracy was found by incorporating air pressure and temperature directly into an advanced space–time statistical forecasting model, the trigonometric direction diurnal (TDD) model. This paper proposes to incorporate the geostrophic wind as a new predictor in the TDD model. The geostrophic wind captures the physical relationship between wind and pressure through the observed approximate balance between the pressure gradient force and the Coriolis acceleration due to the Earth's rotation. Based on our numerical experiments with data from West Texas, our new method produces more accurate forecasts than does the TDD model using air pressure and temperature for 1- to 6-hour-ahead forecasts based on three different evaluation criteria. Furthermore, forecasting errors can be further reduced by using moving average hourly wind speeds to fit the diurnal pattern. For example, our new method obtains between 13.9% and 22.4% overall mean absolute error reduction relative to persistence in 2-hour-ahead forecasts, and between 5.3% and 8.2% reduction relative to the best previous space–time methods in this setting.

1. Introduction. Because it is a rich resource that is both green and renewable, wind energy has been developing rapidly worldwide; see the book by Haugen and Musser (2012) on renewable energy and the reviews by Genton and Hering (2007), Zhu and Genton (2012), and Pinson (2013) for more information about wind energy.

Wind power cannot be simply added into current power systems. Rather, its introduction creates costs and inefficiencies in power systems. Because of the high uncertainties, nondispatchable and limited predictability of wind energy, an

Received June 2013; revised May 2014.

[1]This publication is partly based on work supported by Award No. KUS-C1-016-04 made by King Abdullah University of Science and Technology (KAUST).

[2]Supported in part by NSF Grant DMS-10-07504.

Key words and phrases. Geostrophic wind, space–time statistical model, wind energy, wind speed forecasting.

increase in the proportion of wind power in a system requires a corresponding increase of fast but expensive nonwind backup power to balance wind fluctuations.

The solution to reducing the uncertainties of wind power generation is accurate wind forecasting. In particular, short-term forecasting up to a few hours ahead is essential. Long-term wind forecasting is less accurate, while high-quality short-term prediction is possible. In order to describe the uncertainty in the forecast of a future event, the forecast ought to be probabilistic, that is, in the form of a predictive probability distribution; see Gneiting and Katzfuss (2014) for an overview.

At the same time, short-term forecasting is closely related to a power system dispatch. In a power market, one-day-ahead, hours-ahead, and even minutes-ahead price adjustments are used to determine how much electricity each power plant should generate to meet demand at minimum cost; see Xie et al. (2011). Moreover, if there is a gap between the demand and the estimated supply, there is enough time to draw on less expensive backup power plants. Accurate short-term forecasts reduce the cost for reserves and stabilize the power system.

A number of short-term, statistical, wind forecasting models have been developed; see reviews by Giebel et al. (2011), Kariniotakis et al. (2004), Monteiro et al. (2009), Zhu and Genton (2012) and Pinson (2013). Statistical space–time forecasting models that take into account both spatial and temporal correlations in wind have been found to be particularly accurate for short-term forecasting problems. The regime-switching space–time diurnal (RSTD) models, proposed by Gneiting et al. (2006), were found to outperform persistence (PSS), autoregressive and vector autoregressive models. Since the RSTD models were introduced, researchers have sought to generalize and improve them. For example, Hering and Genton (2010) proposed the trigonometric direction diurnal (TDD) model to generalize the RSTD model by treating wind direction as a circular variable and including it in their model. Zhu et al. (2014) generalized the RSTD model by allowing forecasting regimes to vary with the prevailing wind and season, obtaining comparable forecasting accuracy. They referred to their model as a rotating RSTD model. Pinson and Madsen (2012) used a first-order Markov chain to determine the regime sequence in offshore wind power forecasting problems and proposed the so-called adaptive Markov-switching autoregressive models.

All of the aforementioned statistical wind forecasting models use only historical wind information—wind speed and direction—to predict future winds. Other atmospheric parameters, such as temperature and pressure, are closely tied to the wind through various physical processes and could potentially be included in models to improve prediction accuracy. Directly incorporating temperature and pressure as statistical predictors turns out not to be helpful, however, because winds, for example, are related more closely to horizontal gradients of pressure rather than pressure itself. Outside the tropics, the wind field is closely tied to the large-scale

atmospheric pressure field through a balance between the horizontal pressure gradient force and the Coriolis acceleration from the Earth's rotation. This relationship is known as geostrophic balance [e.g., Wallace and Hobbs (2006), Section 7.2]. Because of the physical relationship between pressure gradients and winds, the atmospheric pressure field contains information about the wind that is not contained in surface wind measurements. For a general introduction to meteorological basics of wind power generation, see Emeis (2013) and the references therein. In this paper, a new predictor is introduced to the TDD model, the geostrophic wind (GW), which is the theoretical horizontal wind velocity that exactly balances the observed pressure gradient force. This new model is named TDDGW.

Numerical experiments applying the TDDGW model to data from West Texas are carried out for 1- to 6-hour-ahead wind forecasting. The geostrophic wind direction (D) and the difference in temperature (T) between the current and previous day are also considered, with corresponding models named TDDGWD and TDDGWT, respectively. Additionally, simpler but more efficient methods are proposed to fit the prevailing diurnal wind pattern to obtain better forecasts. Mean absolute errors (MAE), root mean squared errors (RMSE) and continuous ranked probability scores (CRPS), as well as probability integral transform histograms, are used to evaluate the performance of the forecasting models.

The remainder of this paper is organized as follows. In Section 2 the geostrophic wind estimation procedure is briefly introduced. In Section 3 the TDDGW model is proposed, along with the TDDGWD and TDDGWT models and modified diurnal pattern fitting methods. The West Texas data are used as a case study in Section 4. In Section 5 forecast results are evaluated and compared with those from reference models. Section 6 offers final remarks. The abbreviations used in the paper are listed in Table 1.

2. Estimating the geostrophic wind. Using pressure as a vertical coordinate, the eastward and northward components of the geostrophic wind, u_g and v_g, are given by

$$u_g = -\frac{g_0}{f}\frac{\partial Z}{\partial y} \quad \text{and} \quad v_g = \frac{g_0}{f}\frac{\partial Z}{\partial x}, \tag{1}$$

where x and y are local eastward and northward Cartesian coordinates, g_0 is the acceleration of gravity, $f = 2\Omega \sin\phi$ is the Coriolis parameter, ϕ is latitude, Ω is the rotation rate of the Earth, and Z is the height of a convenient nearby surface of constant pressure.

For the region covered by this study, differences in Z between stations are small [$O(10\,\text{m})$] compared to the magnitude of Z [$O(1000\,\text{m})$], so care must be taken to remove systematic biases and noise in individual measurements of Z to accurately estimate the horizontal pressure gradient. To compute the geostrophic wind components from a network of surface pressure observing stations, the following steps are used. First, because the barometers at different stations are typically located

TABLE 1
List of abbreviations

y	Wind speed
θ	Wind direction
w_g	Geostrophic wind speed
θ_g	Geostrophic wind direction
PSS	Persistence
RSTD	Regime switching space–time diurnal model
TDD	Trigonometric direction diurnal model
TDDGW	TDD model incorporating geostrophic wind information
TDDGWT	Including 24-hour temperature difference into TDDGW
TDDGWD	Including geostrophic wind direction into TDDGW
TDDGWDT	Including 24-hour temperature difference and geostrophic wind direction into TDDGW
YMD	Modified diurnal pattern fitted with yearly period
SMD	Modified diurnal pattern fitted with seasonal period
MD	Modified diurnal pattern fitted with 45 days' period

at different elevations above sea level, it is necessary to adjust the pressure measurements to a standard reference pressure. This can be done with good accuracy through the hydrostatic equation, which in integral form is written as

$$Z = Z_i + \frac{R\bar{T}}{g_0} \ln\left(\frac{p_i}{p_{\text{ref}}}\right), \tag{2}$$

where Z_i is the geopotential height of barometer i, p_i is the pressure measurement by barometer i, p_{ref} is the desired reference pressure level (e.g., 850 hPa), Z is the unknown geopotential height of the reference pressure level, R is the gas constant for air (287 J K^{-1} kg^{-1}), and $\bar{T}$ is the layer-averaged temperature between p_i and p_{ref}, which in this paper is estimated using surface temperature measurements.

Because $\Delta Z/Z \ll 1$ for horizontal scales of interest in this study, systematic biases and random noise in the barometers would lead to large errors in estimates of the pressure gradient. Biases are removed by subtracting the time-mean pressure at each station for the time series. This will also remove any real time-mean geostrophic wind, but for statistical wind forecasting purposes, only variations in the geostrophic wind are of interest. Random noise in the pressure measurements are removed by fitting a smooth (planar) surface,

$$Z(x, y) = a_0 + a_1 x + a_2 y, \tag{3}$$

to the geopotential heights at each time. From this, we get

$$\frac{\partial Z}{\partial x} = a_1 \quad \text{and} \quad \frac{\partial Z}{\partial y} = a_2,$$

which can be substituted into equation (1) to give

$$u_g = -\frac{g_0}{f} a_2 \quad \text{and} \quad v_g = \frac{g_0}{f} a_1. \tag{4}$$

The geostrophic wind speed and direction are given by $w_g = \sqrt{u_g^2 + v_g^2}$ and $\theta_g = \tan^{-1}(v_g/u_g)$, respectively.

3. The trigonometric direction diurnal model with geostrophic wind.

3.1. *The TDD model and reference models.* The TDD model [Hering and Genton (2010)] is an advanced space–time model for short-term wind speed forecasting problems. It generalizes the RSTD model [Gneiting et al. (2006)] by treating wind direction as a circular variable and including it in the model, such that the alterable and locally dependent forecasting regimes are eliminated. The main idea of this model is presented in this section in order to develop our new model.

Let $y_{s,t}$ and $\theta_{s,t}$, $s = 1, \ldots, S$ and $t = 1, \ldots, T$, be surface wind speed and direction measurements at station s at time t, respectively. The objective is to predict the k-step-ahead wind speed, $y_{i,t+k}$, at one of the stations, $i \in \{1, \ldots, S\}$. For short-term wind speed forecasting problems, the k-step-ahead is from 1 to 6 hours.

Like Gneiting et al. (2006) and Hering and Genton (2010), it is assumed in the TDD model that $y_{s,t+k}$ follows a truncated normal distribution, $N^+(\mu_{s,t+k}, \sigma_{s,t+k})$, with $\mu_{s,t+k}$ and $\sigma_{s,t+k}$ as the center parameter and the scale parameter, respectively, considering that the density of the wind speed is nonnegative. Of course, there are other alternative probability distributions to fit wind speed, such as the Weibull, Rayleigh and Beta distributions; see Monahan (2006), Monahan et al. (2011) and Zhu and Genton (2012).

If the two parameters of the truncated normal distribution are modeled appropriately, accurate probabilistic forecasts can be achieved beyond point forecasts. In the TDD model, these two parameters are modeled as follows, taking $s = 1$ as an example:

(a) The center parameter, $\mu_{1,t+k}$, is modeled in two parts:

$$\mu_{1,t+k} = D_{1,t+k} + \mu^r_{1,t+k}.$$

The first part, $D_{1,t+k}$, is the diurnal component in the wind speed, which is fitted by two pairs of trigonometric functions:

$$\begin{aligned} D_{1,h} = {} & d_0 + d_1 \sin\left(\frac{2\pi h}{24}\right) + d_2 \cos\left(\frac{2\pi h}{24}\right) \\ & + d_3 \sin\left(\frac{4\pi h}{24}\right) + d_4 \cos\left(\frac{4\pi h}{24}\right), \end{aligned} \tag{5}$$

where $h = 1, 2, \ldots, 24$.

The residual of the wind speed after removing the diurnal component is modeled as

$$\mu^r_{1,t+k} = \alpha_0 + \sum_{s=1,\ldots,S} \Bigg[\sum_{j=0,1,\ldots,q_s} \alpha_{s,j} y^r_{s,t-j} + \sum_{j'=0,1,\ldots,q'_s} \{\beta_{s,j'} \cos(\theta^r_{s,t-j'}) + \gamma_{s,j'} \sin(\theta^r_{s,t-j'})\} \Bigg]. \tag{6}$$

Equation (6) models the k-step-ahead wind speed residual as a linear combination of current and past wind speed residuals at all stations up to time lag q_s depending on station s, as well as a pair of trigonometric functions of wind direction residuals whose diurnal patterns are also fitted by the model in (5) up to time lag q'_s, which is not necessarily equivalent to q_s. Both q_s and q'_s are determined by the modified Bayesian information criterion (BIC) as described by Hering and Genton (2010).

(b) The scale parameter is modeled by a simple linear model of volatility value, v^r_t, in the following form:

$$\sigma_{1,t+k} = b_0 + b_1 v^r_t,$$

where $v^r_t = \{\frac{1}{2S} \sum_{s=1}^{S} \sum_{l=0}^{1} (y^r_{s,t-l} - y^r_{s,t-l-1})^2\}^{1/2}$ and $b_0, b_1 > 0$.

The coefficients in the center parameter and scale parameter models are estimated numerically by minimizing the continuous ranked probability score (CRPS) for a truncated normal distribution, based on a 45-day-sliding window; see Gneiting et al. (2006) and Gneiting and Raftery (2007).

Two models are introduced briefly here as references:

(i) PSS assumes the future wind speed is the same as the current wind speed, $\hat{y}_{s,t+k} = y_{s,t}$.

(ii) As mentioned above, in the RSTD model [Gneiting et al. (2006)], forecasting regimes are defined based on the prevailing wind direction, and for each regime a separate model is fitted only with historical wind speeds as predictors in equation (6) plus speeds from neighboring stations.

3.2. *The TDDGW model.* Based on the discussion of the geostrophic wind in Section 2, it is clear that atmospheric pressure and temperature play important roles in wind speed and direction. To reduce the uncertainties in wind, an efficient short-term forecasting model should include this critical information. However, the experiments in the next section show that incorporating air pressure and temperature directly into the TDD model does not reduce errors in forecasts. This is because in the TDD model, particularly in the mean structure in equation (6), linearity is assumed between future wind speeds and the covariates. This assumption is invalid between wind speed and air pressure or temperature. As a result, no

improvement is achieved by incorporating these variables directly into the TDD model.

Instead of seeking nonlinear forms between wind speeds and air pressure and temperature in the mean structure of the TDD model, it is proposed to use the geostrophic wind as a predictor, as this better expresses the physical relationship between temperature, pressure and wind. In the TDDGW model, geostrophic wind is incorporated into the TDD model, hence keeping the model structure almost the same. Specifically, the TDD model is modified by adding geostrophic wind into the center parameter model in equation (6):

$$\begin{aligned}\mu^r_{1,t+k} = \alpha_0 + \sum_{s=1,\ldots,S}\Bigg[&\sum_{j=0,1,\ldots,q_s} \alpha_{s,j}\, y^r_{s,t-j} \\ &+ \sum_{j'=0,1,\ldots,q'_s} \{\beta_{s,j'} \cos(\theta^r_{s,t-j'}) + \gamma_{s,j'} \sin(\theta^r_{s,t-j'})\}\Bigg] \\ &+ c_0 (w_g)^r_{1,t} + c_1 (w_g)^r_{1,t-1} + c_2 (w_g)^r_{1,t-2} + \cdots + c_q (w_g)^r_{1,t-q},\end{aligned} \tag{7}$$

where q is the time lag of geostrophic wind depending on the station, s, determined by the aforementioned modified BIC method and, again, w_g indicates the geostrophic wind speed. Since geostrophic wind is the theoretical wind above the planetary boundary layer in the atmosphere, its value for a small area is almost constant. This is why the geostrophic wind is used as a common predictor in equation (7).

In addition to including geostrophic wind in the TDD model, the geostrophic wind direction and the temperature difference between the current and previous day are also considered, because, from the atmospheric science point of view, these variables are closely related to surface wind. These two modified TDDGW models are named TDDGWD and TDDGWT, and with the two variables simultaneously, TDDGWDT.

Additionally, the diurnal pattern fitting is also modified. Instead of the daily wind pattern in the model in equation (5), the average wind speed of each hour within a certain period is treated as the diurnal pattern. Depending on the period used, there are several versions of the diurnal pattern modeling: MD, a diurnal pattern that takes into account winds in a 45-day-sliding window; SMD, a diurnal pattern that is calculated for each season; and YMD, a diurnal pattern based on a whole year's data (or several years' data).

4. West Texas data.

4.1. *Data description*. The wind data considered here were collected from mesonet towers at a height of 10 m above the surface in West Texas and Eastern New Mexico, and was also used by Xie et al. (2014). The original data archive

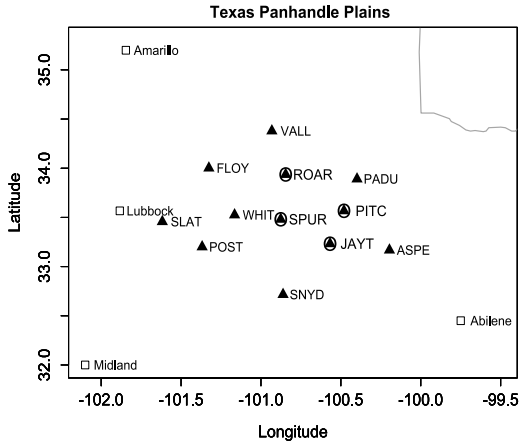

FIG. 1. *The distribution of selected mesonet towers* (*triangles*) *in West Texas* (*Panhandle plains*). *The four towers of PICT, JAYT, SPUR and ROAR are marked by circled triangles. The* 12 *stations selected to estimate the geostrophic wind are marked by triangles.*

contains five-minute means of three-second measurements of wind and other atmospheric parameters from more than 60 stations. In the experiment, hourly-averaged data of five-minute means from 1 January 2008 to 31 December 2010 are used, divided into training data (2008–2009) and testing data (2010). Although most wind turbine towers today are at least 60 m tall [Busby (2012)], winds at 10 m height provide some information about the wind at turbine height depending on the state of the planetary boundary layer. Moreover, we are using 10 m winds because it is all that is available from this data set.

In our numerical experiment, a small area in the Panhandle plains is chosen with four stations to test the newly proposed model; see Figure 1. This area includes PICT, JAYT, SPUR and ROAR stations in and around Dickens county, between 40 to 55 miles apart from one another. These four locations are marked by a circled triangle in Figure 1. Our goal is to predict 1- to 6-hour-ahead wind speeds at these four locations. The recorded data include wind speed, wind direction, temperature and pressure. To estimate the geostrophic wind in the TDDGW model, 12 surface stations were selected (triangles in Figure 1) that surround the four test stations. More information is given at http://www.mesonet.ttu.edu/wind.html.

The area where the four target stations are located in West Texas has both northerly and southerly prevailing winds as shown by Xie et al. (2014) with wind roses based on the 2008–2009 training data set. High frequencies and large speed ranges are found from the north and south directions at all four stations. More specifically, the southerly wind dominates this area, with more frequent wind blowing from the south than from the north. Different from the other three locations, the station SPUR has a high frequency from the northwest direction. The wind speed marginal density plots at the four stations are displayed in Figure 2 based on the wind data from 2008 and 2009. They are positive and skewed to the right.

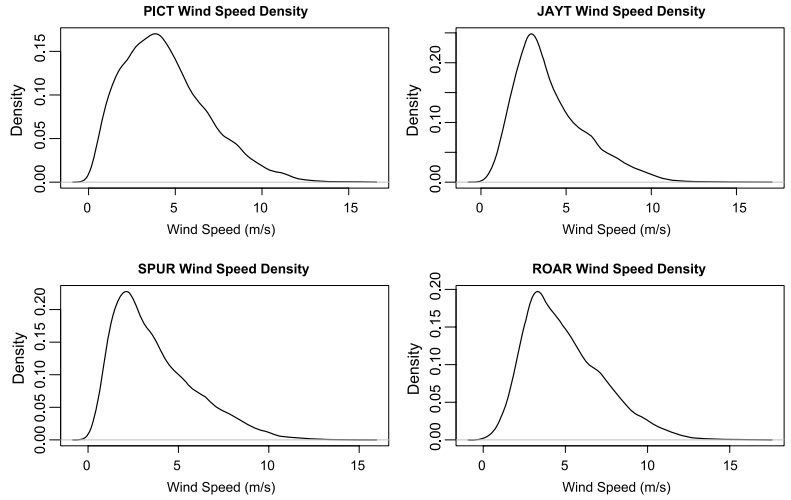

FIG. 2. *Marginal density plots of wind speeds at PICT, JAYT, SPUR and ROAR in* 2008–2009.

4.2. *Geostrophic wind and surface wind.* To estimate the geostrophic wind based on surface measurements of air pressure and temperature, the aforementioned two steps in Section 2 are carried out. First, for each hour, surface pressure measurements are represented by the geopotential height with equation (2). For the value of $\bar{T}$, the average temperature from the 12 stations in Figure 1 is used and 850 hPa for the reference pressure, p_{ref}. Second, using the 12 stations' geopotential height data, along with their latitude and longitude data, a geopotential height plane (3) is fitted for each hour, resulting in a geopotential height gradient based on the coefficients of the plane of the x and y horizontal components as shown in equation (4). The monthly average geopotential height is removed before fitting the plane. With these two steps, each hourly surface wind record has a corresponding geostrophic wind estimated from the temperature and pressure information.

The four days' hourly geostrophic wind speeds (solid curve) and surface winds (dashed curve) in 2008 at PICT in Figure 3 (top) indicate that the former has larger values than the latter, while the latter has larger amplitude of variation. Since the effects of friction forces, which slow down the wind speed and change direction, are ignored in the geostrophic balance, the geostrophic winds are stronger and smoother than the surface winds. Also, it can be seen in Figure 3 that they share similar patterns, which is consistent with the large positive correlation coefficient between the surface wind and the geostrophic wind as listed in Table 2 in the next section. The bottom plot displays the density estimations of the geostrophic wind speed (solid curve) and the surface wind speed (dashed curve), from which we can see again that the geostrophic wind speed has a larger range than does the surface wind speed.

Figure 4 displays scatter plots of wind speed vs. surface temperature (left), pressure (middle) and geostrophic wind speed (right) based on the training data at

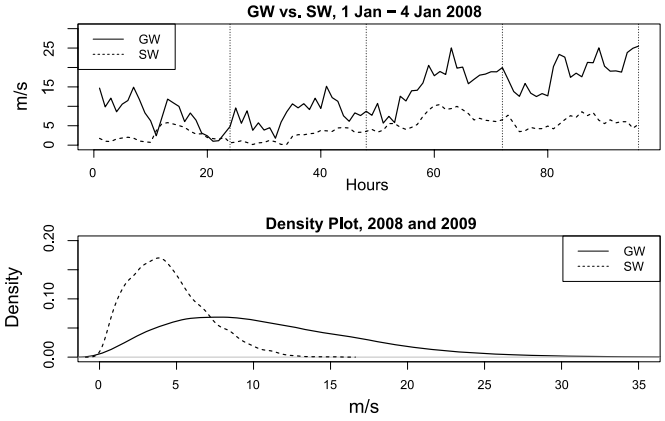

FIG. 3. *Geostrophic wind* (*GW*) *vs. surface wind* (*SW*) (*top*) *and density plots of the geostrophic wind and surface wind* (*bottom*).

PICT. From the first plot, we can see that the surface wind speed is very weakly correlated with temperature. The correlation coefficient between them is 0.19. The correlation coefficient of the surface wind speed and pressure is -0.34, indicating a weakly negative linear trend in the scatter plot as well. However, the linearity correlation between surface wind and geostrophic wind is stronger, with correlation coefficient equal to 0.53. This shows that geostrophic wind not only contains important temperature and pressure information, but also meets the linearity assumption such that it can be integrated into the TDD model. More importantly, geostrophic wind has physical interpretability.

Figure 5 shows the averaged diurnal pattern of the surface wind speed and geostrophic wind in different seasons of 2008–2009 at PICT (left) and ROAR (right). The plots show that geostrophic wind has higher speed than surface wind, which is slowed down by the ground friction. The geostrophic wind for the two stations is the same, but the surface winds are different albeit similar. Through the

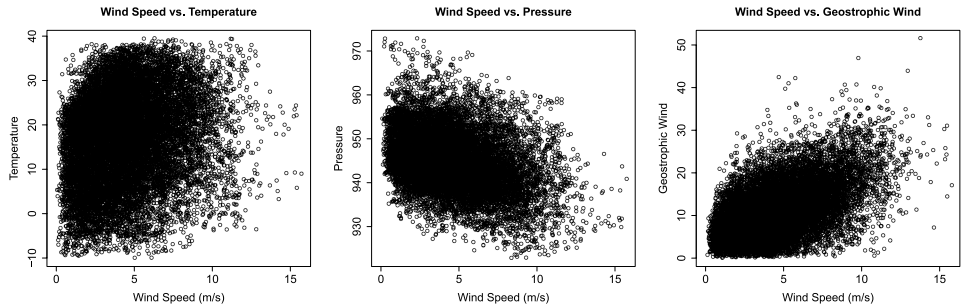

FIG. 4. *Scatter plots of wind speed vs. temperature* (*Celsius*) (*left*), *pressure* (*hPa*) (*middle*) *and geostrophic wind speed* (m/s) (*right*).

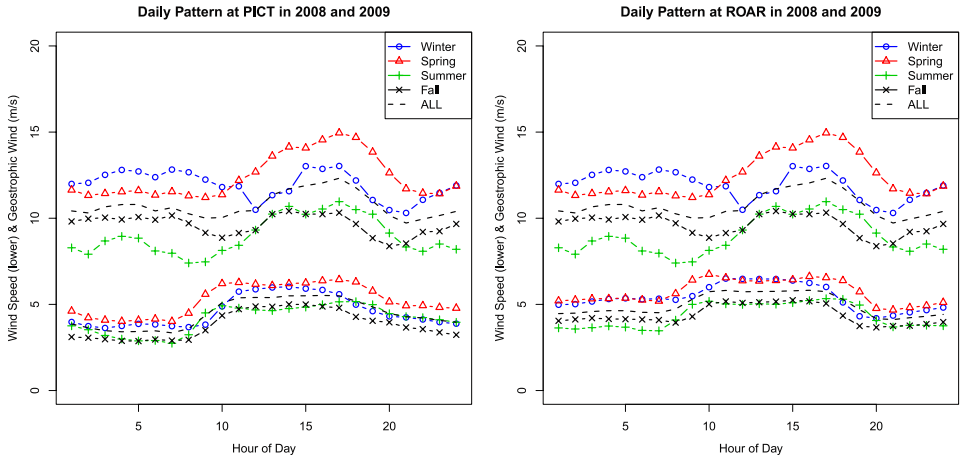

FIG. 5. *Daily pattern of wind speed* (*lower part in each plot*) *and geostrophic wind speed* (*upper part in each plot*) *in different seasons of* 2008–2009 *at PICT* (*left*) *and ROAR* (*right*).

hours of the day, the geostrophic wind fluctuates with a range from 7 to 15 m/s, while the surface wind is smoother with a range from 3 to 6 m/s. Seasonally, geostrophic wind and surface wind are consistent, having higher speed during winter (December to February) and spring (March to May) than summer (June to August) and fall (September to November).

5. Numerical results.

5.1. *Training results*. In the training procedure the models for the center parameter are obtained based on the training data set to forecast 1- to 6-hour-ahead wind speed at each of the four stations. For example, to predict $y_{P,t+2}$, the 2-hour-ahead wind speed at PICT, the variables listed in Table 2, except geostrophic wind direction, are put into the selection pool, and the aforementioned BIC is applied to select significant predictors. The variables in the selection pool include current and up to 10-step lags of wind speed, geostrophic wind speed, and pairs of cosine and sine of the wind direction at all four stations. In the TDDGWD model, the cosine and sine of the geostrophic wind direction are also considered. Different from the cosine and sine of the surface wind direction, which have negative correlations with the 2-hour-ahead wind speed at PICT, the cosine and sine of the geostrophic wind direction are positively correlated with the 2-hour-ahead wind speed at PICT (see Table 2). In the table, the indexes, P, J, S and R, indicate the four locations.

5.2. *Evaluation of forecasts*. The trained TDDGW, TDDGWT, TDDGWD and TDDGWDT models are applied to the testing data set with modified diurnal modeling, MD, SMD and YMD, to predict probabilistically 1- to 6-hour-ahead wind speeds at the four stations. Prediction mean absolute errors (MAE)

TABLE 2

Correlation coefficients between $y_{P,t+2}$ and the current and up to 5-step lag surface wind speed (y), direction (θ), geostrophic wind speed (w_g) and geostrophic wind direction (θ_g) at four stations (P, J, S and R)

Variable	t	$t-1$	$t-2$	$t-3$	$t-4$	$t-5$
y_P	0.80	0.70	0.62	0.54	0.47	0.40
$w_{g,P}$	0.57	0.55	0.53	0.50	0.47	0.43
$\cos(\theta_P)$	−0.06	−0.08	−0.11	−0.13	−0.15	−0.17
$\sin(\theta_P)$	−0.14	−0.16	−0.17	−0.19	−0.20	−0.20
$\cos(\theta_{g,P})$	0.10	0.09	0.09	0.09	0.10	0.10
$\sin(\theta_{g,P})$	0.17	0.15	0.13	0.11	0.09	0.07
y_J	0.74	0.66	0.58	0.51	0.45	0.39
$\cos(\theta_J)$	−0.12	−0.14	−0.15	−0.16	−0.17	−0.18
$\sin(\theta_J)$	−0.14	−0.17	−0.19	−0.21	−0.22	−0.23
y_S	0.73	0.64	0.55	0.48	0.40	0.33
$\cos(\theta_S)$	−0.19	−0.20	−0.20	−0.20	−0.20	−0.20
$\sin(\theta_S)$	−0.06	−0.09	−0.11	−0.14	−0.16	−0.18
y_R	0.76	0.70	0.64	0.59	0.53	0.48
$\cos(\theta_R)$	−0.03	−0.04	−0.06	−0.08	−0.10	−0.12
$\sin(\theta_R)$	−0.05	−0.08	−0.11	−0.13	−0.16	−0.17

are used to evaluate the performance of the forecasts, which are defined as $\sum_{t=1}^{T} |y_{P,t+2} - \hat{y}_{P,t+2}|$, at station PICT for 2-hour-ahead, for example. When $\hat{y}_{P,t+2}$ equals to the median of the predictive distribution, the error reaches the minimum value. Thus, for the truncated normal distribution, we take the median as forecast:

$$\hat{y}_{P,t+2} = \mu_{P,t+2} + \sigma_{P,t+2} \cdot \Phi^{-1}\{0.5 + 0.5 \cdot \Phi(-\mu_{P,t+2}/\sigma_{P,t+2})\};$$

see Gneiting (2011) for a discussion of quantiles as optimal point forecasts. A 45-day-sliding window is used to estimate the coefficients in the models with the CRPS method. Forecasts are compared with the reference models listed in Section 3.1 in addition to the TDD model.

Besides MAE, the RMSE and CRPS are also used to compare model performance. Compared with MAE, RMSE has stronger penalty on large forecast errors. CRPS essentially provides a measure of probabilistic forecast performance. The computation of the CRPS for the truncated normal distribution can be found in Gneiting et al. (2006).

In Table 3 the prediction MAE values of 2-hour-ahead forecasts at PICT in 2010 from the TDDGW model with aforementioned different diurnal modeling methods are listed. Overall, the MD method has the smallest MAE values among the four, 0.88 m/s compared with 0.92 m/s, 0.89 m/s and 0.90 m/s, from TDDGW, TDDGW-SMD and TDDGW-YMD methods, respectively. The TDDGW-

TABLE 3
MAE values (m/s) of 2-hour-ahead forecasts from TDDGW with different diurnal component fitting methods at PICT in 2010. The smallest MAE value of each column is boldfaced

Site	Model	Jan.	Feb.	Mar.	Apr.	May	Jun.	Jul.	Aug.	Sep.	Oct.	Nov.	Dec.	Overall
PICT	TDDGW	0.95	0.81	1.02	0.93	**0.91**	0.96	0.91	0.91	0.84	0.82	0.97	0.98	0.92
PICT	TDDGW-MD	**0.94**	**0.80**	**0.96**	0.89	0.92	**0.91**	**0.83**	**0.86**	0.81	**0.77**	**0.92**	**0.94**	**0.88**
PICT	TDDGW-SMD	**0.94**	0.84	0.98	**0.88**	0.93	0.93	0.85	**0.86**	0.82	0.78	0.94	0.96	0.89
PICT	TDDGW-YMD	0.98	0.81	0.98	0.91	0.95	0.96	0.86	0.88	**0.80**	0.81	0.96	0.98	0.90

MD model has the smallest MAE values, 10 out of the 12 months, followed by TDDGW-SMD, 3 out of 12 months.

The modified methods fit the diurnal pattern better than the one in equation (5). This is because the latter fits the pattern by a continuous smooth function of the time of a day. The fitted results would be adjusted to the average wind speed of the day, while MD, SMD and YMD only provide the average wind speed on the hours. Since the focus is on hourly ahead forecasting, here using MD, SMD and YMD is reasonable without losing functionality in practice. Therefore, in the following only forecasts from models that use the MD method to fit the diurnal component are displayed.

The MAE, RMSE and CRPS values of 2-hour-ahead forecasts from different models at PICT in 2010 are listed in Table 4. At PICT, it can be observed that all the space–time models outperform the PSS model as expected, with smaller MAE values. Except for February, our new models that incorporate geostrophic wind give more accurate forecasts than the RSTD and TDD models do, with the MAE value 0.88 m/s compared with 0.94 m/s and 0.95 m/s. Up to two decimal points, the TDDGW-MD, TDDGWT-MD, TDDGWD-MD and TDDGWDT-MD models have similar MAE values, around 0.88 m/s. Looking more closely, the TDDGWD-MD gives the largest reduction in the relative MAE value, around 18.3%. As expected, the models including geostrophic wind are better than the other two space–time models (RSTD and TDD) with 13.2% and 12.1% reductions in MAE values relative to PSS. Comparing the results of the TDDGW and TDDGW-MD models, the modified diurnal pattern modeling based on the 45-day-sliding window helps to provide a 3.7% reduction in the MAE value relative to PSS. Similar results can be seen based on CRPS and RMSE. Our new models produce the smallest CRPS and RMSE.

Looking across the 4 locations, our new method obtains between 13.9% and 22.4% overall mean absolute error reduction relative to persistence in 2-hour-ahead forecasts, and between 5.3% and 8.2% reduction relative to the best previous space–time methods in this setting.

To assess calibration, we display the histograms of the probability integral transform (PIT) of our models in Figure 6 for 2-hour-ahead forecasts at PICT in 2010.

TABLE 4

MAE, RMSE and CRPS values (m/s) of 2-hour-ahead forecasts from various forecasting models at PICT in 2010. The smallest value of each criteria in each column is boldfaced

Site	Model	Jan.	Feb.	Mar.	Apr.	May	Jun.	Jul.	Aug.	Sep.	Oct.	Nov.	Dec.	Overall
MAE														
PICT	PSS	1.06	0.87	1.21	1.15	1.15	1.13	1.03	1.05	0.96	0.97	1.17	1.14	1.08
PICT	RSTD	0.93	**0.79**	1.07	0.98	1.02	0.95	0.89	0.90	0.83	0.82	0.99	1.01	0.94
PICT	TDD	0.95	0.81	1.07	0.99	1.00	0.97	0.89	0.93	0.84	0.86	1.01	1.03	0.95
PICT	TDDGW-MD	0.94	0.80	**0.96**	**0.89**	**0.92**	0.91	**0.83**	**0.86**	0.81	**0.77**	**0.92**	**0.94**	**0.88**
PICT	TDDGWT-MD	0.94	0.82	**0.96**	0.90	**0.92**	0.91	**0.83**	**0.86**	0.81	**0.77**	**0.92**	0.95	**0.88**
PICT	TDDGWD-MD	**0.91**	0.82	0.97	**0.89**	**0.92**	**0.90**	0.84	**0.86**	**0.80**	0.78	**0.92**	**0.94**	**0.88**
PICT	TDDGWDT-MD	**0.91**	0.83	0.97	0.90	**0.92**	**0.90**	0.84	**0.86**	**0.80**	0.78	**0.92**	**0.94**	**0.88**
RMSE														
PICT	PSS	1.45	1.19	1.66	1.54	1.52	1.52	1.40	1.44	1.30	1.31	1.63	1.56	1.47
PICT	RSTD	1.25	**1.05**	1.40	1.29	1.35	1.25	1.20	1.16	1.09	1.07	1.30	1.35	1.24
PICT	TDD	1.25	1.07	1.41	1.28	1.31	1.26	1.19	1.21	1.09	1.09	1.31	1.38	1.25
PICT	TDDGW-MD	1.23	**1.05**	**1.28**	**1.15**	**1.22**	1.22	1.13	**1.12**	1.05	**1.02**	1.21	**1.28**	**1.17**
PICT	TDDGWT-MD	1.23	1.07	**1.28**	**1.15**	**1.22**	**1.21**	**1.12**	**1.12**	1.05	**1.02**	**1.20**	**1.28**	**1.17**
PICT	TDDGWD-MD	**1.20**	1.08	1.29	**1.15**	1.23	1.22	**1.12**	1.13	**1.03**	**1.02**	1.21	**1.28**	**1.17**
PICT	TDDGWDT-MD	1.21	1.09	1.29	1.16	1.23	**1.21**	**1.12**	1.13	**1.03**	**1.02**	1.21	**1.28**	**1.17**
CRPS														
PICT	RSTD	0.67	**0.57**	0.77	0.71	0.73	0.68	0.65	0.64	0.59	0.59	0.71	0.72	0.67
PICT	TDD	0.68	0.58	0.77	0.71	0.71	0.69	0.64	0.67	0.60	0.61	0.72	0.74	0.68
PICT	TDDGW-MD	0.66	0.58	**0.70**	**0.64**	**0.66**	**0.65**	**0.60**	0.62	0.58	0.56	**0.66**	**0.68**	**0.63**
PICT	TDDGWT-MD	0.66	0.59	**0.70**	**0.64**	**0.66**	**0.65**	**0.60**	**0.61**	0.58	**0.55**	**0.66**	**0.68**	**0.63**
PICT	TDDGWD-MD	**0.65**	0.59	**0.70**	**0.64**	**0.66**	**0.65**	**0.60**	0.62	**0.56**	0.56	0.67	**0.68**	**0.63**
PICT	TDDGWDT-MD	**0.65**	0.60	**0.70**	**0.64**	**0.66**	**0.65**	**0.60**	0.62	0.57	0.56	0.67	**0.68**	**0.63**

The PIT is the value attained by the predictive distribution at the observation [Dawid (1984), Diebold, Gunther and Tay (1998)]. We see that all six PIT histograms are approximately uniform, hence indicating calibration and prediction intervals that have close to nominal coverage at all levels. To assess sharpness, we compute the average width of the 90% central prediction intervals. We obtain 3.59 m/s for RSTD and 3.61 m/s for TDD, whereas for the models based on geostrophic wind the values drop to between 3.34 m/s for TDDGW-MD and 3.29 m/s for TDDGWDT-MD, a reduction of forecast uncertainty of about 7–9%.

Figure 7 displays overall MAE values of forecasts from the PSS, RSTD, TDD and TDDGW-MD models for 1- to 6-hour-ahead forecasting at PICT in 2010. We can see that the space–time models improve the forecasting accuracy with smaller MAE values compared to PSS. Our new model has smallest MAE values for all the six forecast horizons. The RSTD and TDD have quite close results. At the same time, as expected, forecasting accuracy decreases with the increase

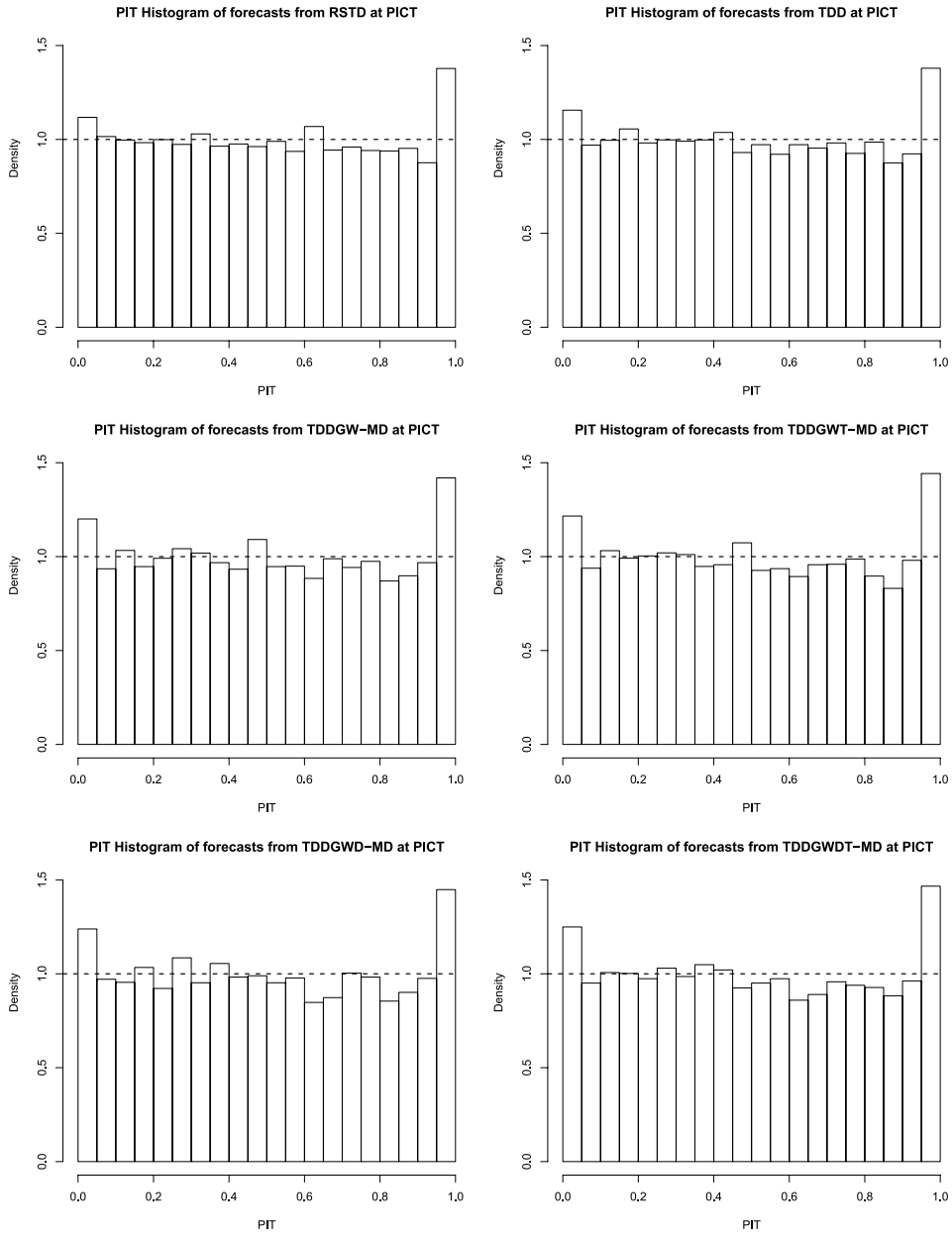

FIG. 6. *PIT histograms for RSTD*, *TDD*, *TDDGW-MD*, *TDDGWT-MD*, *TDDGWD-MD and TDDGWDT-MD predictive distributions of* 2*-hour-ahead forecasts at PICT in* 2010.

of forecasting horizon for all the four models, but the space–time models have a smaller increasing rate than the PSS model. Similar results were obtained with RMSE and CRPS, as well as at other locations.

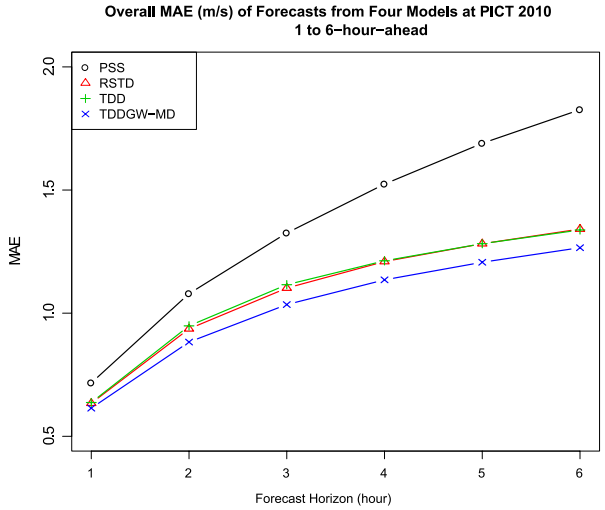

FIG. 7. *Plot of MAE* (m/s) *of forecasts from the PSS, RSTD, TDD and TDDGW-MD models for* 1- *to* 6*-hour-ahead forecasting at PICT in* 2010.

6. Final remarks. Accurate wind prediction is critical in running power systems that have large shares of wind power. In recent decades many studies have been devoted to improving short-term wind forecasting for large-scale wind power development around the world.

This paper developed statistical short-term wind forecasting models based on atmospheric dynamics principles. It proposed the use of the geostrophic wind as a predictor. The geostrophic wind is a good approximation to the winds in the extratropical free troposphere and can be estimated using only surface pressure and temperature data. In terms of the underlying atmospheric physics, the geostrophic wind is correlated to the real wind more strongly than either temperature or pressure. This is demonstrated by the fact that no improvement was found by directly incorporating atmospheric temperature and pressure into the most advanced space–time forecasting model to date. The geostrophic wind can be approximated from networks of standard surface meteorological observations. More importantly, it helps to reduce prediction errors significantly when incorporated into space–time models.

In this paper, more accurate forecasts were achieved by incorporating geostrophic wind as a predictor into space–time statistical models and modifying diurnal pattern models in 1- to 6-hour-ahead wind speed forecasting. In addition, trigonometric functions of the geostrophic wind direction and temperature differences between the current and previous day were also considered. We showed how simpler but more efficient methods can be applied to fit the diurnal pattern of wind to obtain better forecasts.

With our new model and existing space–time models, we forecast the 1- to 6-hour-ahead wind speeds at four locations in West Texas. Three different criteria

were used to evaluate the performance of the models, including MAE, RMSE and CRPS. The results showed that our new models outperform the PSS, RSTD and TDD in terms of all three criteria. Moreover, PIT histograms confirmed that our new models based on geostrophic wind were calibrated and sharp. Xie et al. (2014) further quantified the overall cost benefits on power system dispatch by reducing uncertainties in near-term wind speed forecasts based on the TDDGW model.

Acknowledgments. The authors thank the West Texas Mesonet (www.mesonet.ttu.edu), operated by Texas Tech University, for use of the mesonet meteorological data.

REFERENCES

BUSBY, R. L. (2012). *Wind Power*: *The Industry Grows Up*. PennWell Corporation, Tulsa, OK.

DAWID, A. P. (1984). Statistical theory. The prequential approach. *J. Roy. Statist. Soc. Ser. A* **147** 278–292. MR0763811

DIEBOLD, F. X., GUNTHER, T. A. and TAY, A. S. (1998). Evaluating density forecasts with applications to financial risk management. *Internat. Econom. Rev.* **39** 863–883.

EMEIS, S. (2013). *Wind Energy Meteorology*. Springer, Berlin.

GENTON, M. G. and HERING, A. S. (2007). Blowing in the wind. *Significance* **4** 11–14. MR2359227

GIEBEL, G., BROWNSWORD, R., KARINIOTAKIS, G., DENHARD, M. and DRAXL, C. (2011). The state-of-the-art in short-term prediction of wind power: A literature overview, 2nd ed. ANEMOS.plus, 109 p.

GNEITING, T. (2011). Quantiles as optimal point forecasts. *Int. J. Forecast.* **27** 197–207.

GNEITING, T. and KATZFUSS, M. (2014). Probabilistic forecasting. *Annual Review of Statistics and Its Application* **1** 125–151.

GNEITING, T. and RAFTERY, A. E. (2007). Strictly proper scoring rules, prediction, and estimation. *J. Amer. Statist. Assoc.* **102** 359–378. MR2345548

GNEITING, T., LARSON, K., WESTRICK, K., GENTON, M. G. and ALDRICH, E. (2006). Calibrated probabilistic forecasting at the stateline wind energy center: The regime-switching space-time method. *J. Amer. Statist. Assoc.* **101** 968–979. MR2324108

HAUGEN, D. M. and MUSSER, S. (2012). *Renewable Energy*. Greenhaven Press, Detroit, MI.

HERING, A. S. and GENTON, M. G. (2010). Powering up with space-time wind forecasting. *J. Amer. Statist. Assoc.* **105** 92–104. MR2757195

KARINIOTAKIS, G., PINSON, P., SIEBERT, N., GIEBEL, G. and BARTHELMIE, R. (2004). The state-of-the-art in short-term prediction of wind power-from an offshore perspective. In *Symposium ADEME*, *IFREMER*, *Renewable Energies at Sea*. Brest, FR.

MONAHAN, A. H. (2006). The probability distribution of sea surface wind speeds. Part I: Theory and SeaWinds observations. *J. Climate* **19** 497–520.

MONAHAN, A. H., HE, Y., MCFARLANE, N. and DAI, A. (2011). The probability distribution of land surface wind speeds. *J. Climate* **24** 3892–3909.

MONTEIRO, C., BESSA, R., MIRANDA, V., BOTTERUD, A., WANG, J. and CONZELMANN, G. (2009). Wind power forecasting: State-of-the-art 2009. Technical Report ANL/DIS-10-1, Argonne National Laboratory, US Dept. Energy.

PINSON, P. (2013). Wind energy: Forecasting challenges for its operational management. *Statist. Sci.* **28** 564–585. MR3161588

PINSON, P. and MADSEN, H. (2012). Adaptive modelling and forecasting of offshore wind power fluctuations with Markov-switching autoregressive models. *J. Forecast.* **31** 281–313. MR2924797

WALLACE, J. M. and HOBBS, P. V. (2006). *Atmospheric Science*: *An Introductory Survey*. Elsevier, Boston, MA.

XIE, L., CARVALHO, P., FERREIRA, L., LIU, J., KROGH, B., POPLI, N. and ILIĆ, M. (2011). Wind energy integration in power systems: Operational challenges and possible solutions. *Special Issue of the Proceedings of IEEE on Network Systems Engineering for Meeting the Energy and Environment Dream* **99** 214–232.

XIE, L., GU, Y., ZHU, X. and GENTON, M. G. (2014). Short-term spatio-temporal wind power forecast in robust look-ahead power system dispatch. *IEEE Trans*. *Smart Grid* **5** 511–520.

ZHU, X. and GENTON, M. G. (2012). Short-term wind speed forecasting for power system operations. *Int*. *Stat*. *Rev*. **80** 2–23. MR2990340

ZHU, X., GENTON, M. G., GU, Y. and XIE, L. (2014). Space-time wind speed forecasting for improved power system dispatch. *TEST* **23** 1–25. MR3179610

X. ZHU
DEPARTMENT OF STATISTICS
TEXAS A&M UNIVERSITY
COLLEGE STATION, TEXAS 77843-3143
USA
E-MAIL: email2xzhu@gmail.com

K. P. BOWMAN
DEPARTMENT OF ATMOSPHERIC SCIENCES
TEXAS A&M UNIVERSITY
COLLEGE STATION, TEXAS 77843-3150
USA
E-MAIL: k-bowman@tamu.edu

M. G. GENTON
CEMSE DIVISION
KING ABDULLAH UNIVERSITY OF SCIENCE
AND TECHNOLOGY
THUWAL 23955-6900
SAUDI ARABIA
E-MAIL: marc.genton@kaust.edu.sa